RECENT ADVANCEMENTS IN SPUTTER-TYPE HEAVY NEGATIVE ION SOURCES*

G. D. Alton
P. O. Box 2008, Oak Ridge National Laboratory, Oak Ridge, Tennessee 37831-6368

Abstract

Significant advancements have been made in sputter-type negative ion sources which utilize (1) direct surface ionization, or (2) a plasma to form the positive ion beam used to effect sputtering of samples containing the material of interest. Typically, such sources can be used to generate usable beam intensities of a few μA to several mA from all chemically active elements, depending on the particular source and the electron affinity of the element in question. The presentation will include an introduction to the fundamental processes underlying negative ion formation by sputtering from a low work function surface and several sources will be described which reflect the progress made in this technology.

Introduction

The sputter technique has proved to be a universal method for generating atomic and molecular negative ion beams from chemically active elements. In addition to being versatile in terms of species, sources based on this concept, such as those described in Refs. 1-5, are simple in design, easy to operate, and generally have long lifetimes. Because of these factors, such sources are utilized extensively in most tandem electrostatic accelerator heavy ion physics research laboratories, as well as for use in a growing number of other applications, including high-energy ion implantation and tandem accelerator mass spectrometry. In addition, several heavy ion physics research facilities predicated on the synchrotron principle have been constructed or are under construction. Still other facilities such as the Heavy Ion Storage Ring for Atomic Physics (HISTRAP)[6] at the Oak Ridge National Laboratory are proposed. If funded, the Holifield Heavy Ion Research Facility 25URC tandem electrostatic accelerator would serve as the injector for HISTRAP. For such applications, low duty factor (10^{-4}-10^{-3}), high intensity ($\geq$ 200 μA), pulsed negative ion beams (pulse widths: 50-300 μsec) of a wide variety of negative ion species are typically required from the source. A recently developed, high-brightness, pulsed-mode, plasma sputter negative ion source,[5] appears to be well suited for tandem electrostatic accelerator/synchrotron injection applications.

The present article will provide a brief introduction to the principles of negative ion formation in sources predicated on the sputter principle and a number of sources which are representative of the present state of the art of this technology will be described.

Principles of Negative Ion Formation by Sputtering

The presence of less than a monolayer of a highly electropositive adsorbate material on the surface of a sample undergoing particle bombardment greatly enhances the probability for negative ion formation of sputter-ejected particles.[7] While it is possible that other independent and distinct negative ion formation processes may coexist during sputtering, there is convincing evidence that the mechanism of ion formation during sputtering of a metal surface covered with a partial layer of a material such as cesium is a form of surface ionization. Clear experimental evidence of this mechanism has been provided by Yu,[8] who was able to show a direct correlation between change in work function during adsorption of cesium on clean Mo and the yield of Mo^- ions ejected from the surface during bombardment with a Ne^+ beam. Progress has been made over the past few years toward a quantitative understanding of the secondary negative ion formation process. The process can be formulated in terms of a composite, idealistic, but heuristically useful model such as outlined below.

Negative Ion Generation Rate: If collisional detachment and interference to sputtering of sample atoms by surface adsorbate material effects are ignored, the negative ion current I^- generated by sputtering can be expressed by the following simple relationship:

$$I^- = 2\pi I^+(E_1)\, S(E_1,\theta) \int_{V_i}^{E'} \int_0^{\pi/2} P^-(E_2,\theta)\, f_o(E_2,\theta) \sin\theta d\theta dE_2 . \quad (1)$$

In Eq. 1, I^+ is the incident positive ion current of energy E_1, $S(E_1,\theta_i)$ is the sputter ratio of the target at projectile energy E_1 and angle of incidence with respect to the surface normal θ_i, $f_o(E_2, \theta)$ is the neutral atom energy-angular distribution function and $P^-(E_2,\theta)$ is the probability for negative ion formation of atoms ejected at energy E_2 and polar angle θ with respect to the surface normal. The limits of integration over energy E_2 are taken between V_i, the image potential induced in the surface by the departing negative ion, and E', the maximum energy transfer that can occur between a projectile of energy E_1 and mass M_1 and a target atom of mass M_2. E' is given by the relation $E' = 4M_1M_2E_1/(M_1 + M_2)^2$. The positive ion current I^+ can, in principle, be measured or estimated and the sputter ratio S can be readily calculated by scaling the Sigmund theory[9] into agreement with experiment.

The Probability of Negative Ion Formation: In the prescription of Nørskov and Lundqvist,[10] the probability for negative ion formation during sputtering can be represented by the following simple energy-dependent relation:

$$P^-(E_2,\theta) = \frac{2}{\pi} e^{-\beta\sqrt{M_2}\left\{\phi(\sigma) - E_A + V_i\right\}/\sqrt{2E_2}\cos\theta} . \quad (2)$$

In Eq. 2, ϕ is the work function of the surface which is a function of the relative adsorbate coverage σ, E_A is the electron affinity of the ejected particle of mass M_2 and energy E_2, V_i is the image potential induced in the surface by the escaping ion, θ is the polar angle of the sputtered ion with respect to the surface normal and β is a constant. In Eq. 2, $\sqrt{2E_2/M_2}\cos\theta = v_\perp$, is the component of the velocity of the escaping particle perpendicular to the metal surface. Experimental evidence in support of the velocity dependence of the secondary ion formation process has been provided by Yu for negative ions.[11]

Neutral Particle Energy-Angular Distribution Function: Under the assumption of isotropic collision cascades and a planar surface potential E_b, Thompson[12] derived the following energy-angular distribution function for sputter ejected atoms:

$$f_0(E_2,\theta) = \frac{A_0 E_2 \cos\theta}{(E_2 + E_b)^3} . \quad (3)$$

* Research sponsored by the U.S. Department of Energy under contract DE-AC05-84OR21400 with Martin Marietta Energy Systems, Inc.

In Eq. 3, E_2 is the energy of the ejected particle and θ is the polar angle with respect to the normal of the surface. The maximum in the distribution occurs at $E_{2max} = E_b/2$ and is independent of emission angle θ. The normalization constant A_0, is determined by requiring that the integral $2\pi \int_{V_i}^{E'} \int_0^{\pi/2} f(E_2,\theta) \sin\theta d\theta dE_2 = 1$ where V_i is the image potential induced in the surface by the departing negative ion and E' is given by $E' = 4M_1M_2E_1/(M_1 + M_2)^2$.

Electropositive Adsorbate Effects: It is well known that atomic adsorption of a dissimilar element on a clean surface affects the surface work function.[13] The magnitude and sign of the change depends on the chemical properties of the adsorbed atom (adsorbate) and those of the host material (adsorbent). Electropositive atoms decrease the work function while electronegative atoms tend to increase the work function. Simple analytical expressions have been derived by Alton[14] which can be used to predict, with good accuracy, the value of the work function σ at its minimum and over the complete range ($\sigma = 0$ to $\sigma = 1$) of adsorbate coverage for many alkali and alkaline earth-metal adsorbate-adsorbent combinations. The relationship of Ref. 14 is given by

$$\phi(\sigma) = \phi_0 + \frac{6\Delta\phi_m\sigma}{(3-\sigma_m)\sigma_m} - \frac{3\Delta\phi_m(\sigma_m+1)\sigma^2}{(3-\sigma_m)\sigma_m^2} + \frac{2\Delta\phi_m\sigma^3}{(3-\sigma_m)\sigma_m^2}[V], \quad (4)$$

where ϕ_0 is the intrinsic work function of the surface at $\sigma = 0$ and $\Delta\phi_m$ is the maximum change in work function which occurs at a relative adsorbate coverage value of $\sigma = \sigma_m$.

Total Probability for Negative Ion Formation: In order to determine the total probability for negative ion formation at a particular surface coverage σ, one must integrate the product function formed with Eq. 2 and Eq. 3 over the complete range of particle ejection energy E_2 and over all polar angle θ. Figure 1 displays total probability P_T^- versus cesium surface coverage σ as predicted for Mo^-. The results displayed in Fig. 1 should reflect the correct shape of the total probabilities versus relative cesium adsorbate coverage σ, if not absolute values.

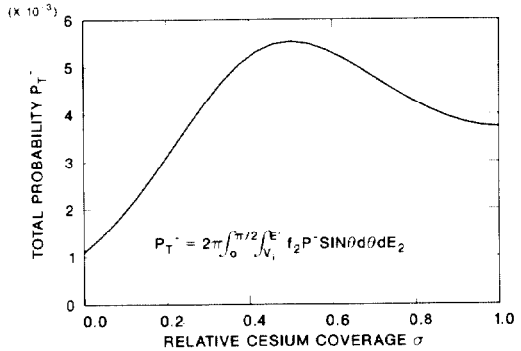

Fig. 1. Total probability P_T^- for Mo^- formation versus relative cesium coverage determined by integrating the product of Eq. 2 and Eq. 3 over the complete range in energy and angle.

Negative Ion Sources Based on Direct Surface Ionization of Cesium Vapor

Sputter-type sources can be categorized according to the means for producing the positive ion beam used to sputter the sample. Several sources utilize direct surface ionization of cesium vapor as it comes in contact with a hot, high-work-function surface to form positive ions which are then accelerated against a negatively biased probe containing the material of interest. The positive ion currents achievable in such sources can attain values up to the space charge limit of the particular electrode configuration. The space charge limited current I^+ which can be accelerated through a potential difference V between the sample and surface ionizer is given by:

$$I^+ = PV^{3/2} \quad (5)$$

where P is the perveance of the particular electrode configuration. The perveance is a function of the geometry of the electrode system and mass M_1 of the bombarding ion species. The perveance can be calculated by the use of computer programs, such as described in Refs. 15 and 16, which solve Poisson's equation for the particular electrode system.

State-of-the-art negative ion sources based on direct surface ionization of cesium are described below. All of the sources were designed and developed at the Oak Ridge National Laboratory.

The source equipped with a spherical geometry ionizer

The space charge limited optics for cesium ion flow in a source equipped with a spherical geometry ionizer is shown schematically in Fig. 2. This source has been described previously[3] and the emittance of the source is reported in Ref. 17. The positive cesium ion beam current density distribution at impact with the sample surface is typically ~ 0.75 mm full diameter when the sample is positioned at the focal point of the system. The computed perveance for cesium in this electrode configuration is $P = 2 \times 10^{-9}$ [$A/V^{3/2}$].

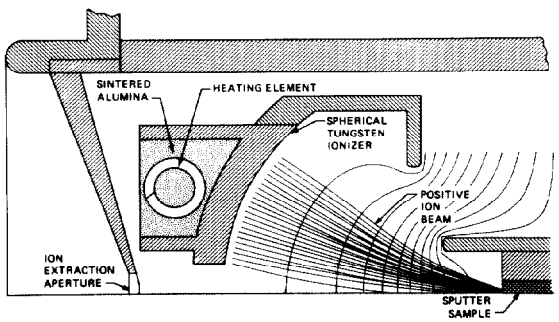

Fig. 2. Positive cesium ion optics for space charge limited flow in the cesium sputter negative ion source equipped with a spherical geometry cesium ionizer (Ref. 3).

The source equipped with an ellipsoidal geometry cesium ionizer

This source is briefly described in Ref. 17. Figure 3 illustrates the optics for space charge limited cesium flow in this highly converging electrode system. When placed at the focal point of the electrode system, the sample wear pattern has a diameter $\phi \cong 1.25$ mm. This electrode configuration has a high perveance in relation to other focusing systems. The computationally determined perveance for the electrode system is found to be $P = 17 \times 10^{-9}$ [$A/V^{3/2}$].

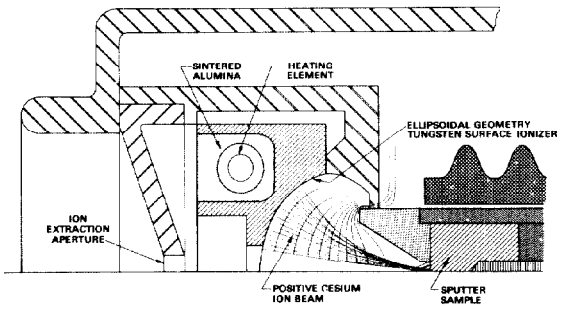

Fig. 3. Positive cesium ion optics for space charge limited flow in the cesium sputter negative ion source equipped with an ellipsoidal geometry cesium ionizer (Ref. 17).

The source equipped with a cylindrical geometry ionizer

The cylindrical geometry ionizer source configuration, shown in Fig. 4, has been described in detail in Refs. 2 and 3 and the emittance and brightness characteristics of the source have been reported in Ref. 17. The observed wear pattern from this source is composed of two parts: a region of concentrated wear with full diameter of ~ 0.75 mm, and a low-density, uniform-wear region with a diameter of ~ 4.5 mm. Because of the greater size of the region of negative ion generation, the emittance of this source is expected to be larger than those of the previously described sources equipped with spherical and ellipsoidal geometry ionizers. The computed perveance of this ionizer geometry for cesium is $P \cong 57 \times 10^{-9}$ [$A/V^{3/2}$].

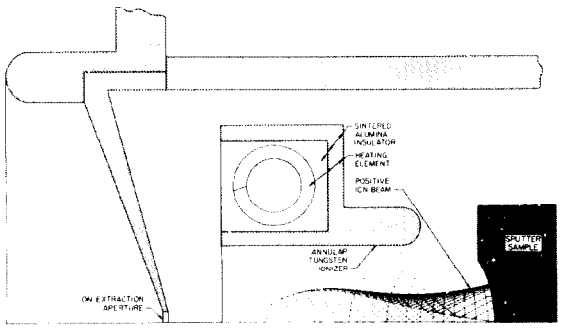

Fig. 4. Positive cesium ion optics for space charge limited flow in the cesium sputter negative ion source equipped with an cylindrical geometry cesium ionizer (Ref. 2).

Negative ion beam intensity data: The versatility of the sources described above is reflected by the wide spectrum of momentum analyzed negative ion beams that have been observed during their operation. A partial list of species and negative ion beam intensities realized from these sources under a variety of operating conditions are the following: 50 μA H^-, 8 μA Li^-, 3 μA BeH_3, 10 μA B^-, 270 μA C^-, 1 μA NH_2, 280 μA O^-, 30 μA F^-, 3 μA Na^-, 12 μA MgH^-, 2.8 μA Al^-, 100 μA Si^-, 1 μA P^-, 100 μA S^-, 30 μA Cl^-, 0.5 μA K^-, 0.4 μA CaH^-, 2 μA ScH^-, 15 μA TiH_3, 4 μA CrH_2, 1 μA MnO^-, 0.6 μA FeO^-, 1 μA Co^-, 6 μA CoO^-, 12 μA Ni^-, 200 μA Cu^-, 1 μA ZnO^-, 4 μA GaO^-, 2 μA Ge^-, 40 μA As^-, 75 μA Se^-, 25 μA Br^-, 0.5 μA Rb^-, 0.6 YO^-, 18 μA ZrH, .4 μA Nb^-, 1.0 μA NbO^-, 1.0 μA MoO^-, 0.5 μA Pd^-, 18 μA Ag^-, 0.5 μA CdO^-, 0.5 μA Sn^-, 0.9 μA Sb^-, 30 μA I^-, 0.2 μA Cs^-, 4 μA TaO^-, 0.7 μA WO^-, 1 μA ReO^-, 0.3 μA Os^-, 5 μA Ir^-, 75 μA Pt^-, 170 μA Au^-, 0.5 μA TlO^-, 0.7 μA Pb^-, 0.6 μA Bi^-, 0.6 μA UC_2.

Emittance data: Average normalized emittance data for these sources are displayed in Fig. 5 as a function of total percent of negative ion beam intensity. The emittance values are defined by the following relations:

$$\varepsilon_{nx} = \pi \int\int dx dx' \sqrt{E} \quad \text{(x-direction)},$$
$$\varepsilon_{ny} = \pi \int\int dy dy' \sqrt{E} \quad \text{(y-direction)},$$
$$\text{and } \varepsilon = (\varepsilon_{nx}.\varepsilon_{ny})^{1/2}. \qquad (6)$$

In Eqs. 6, x, y are position coordinates, x′, y′ are angular coordinates, and E is the energy of the ion beam. Emittance in this prescription is usually given in units of π mm.mrad $(MeV)^{1/2}$. The definitions given by Eqs. 6 are used for the emittances of all sources described in this report.

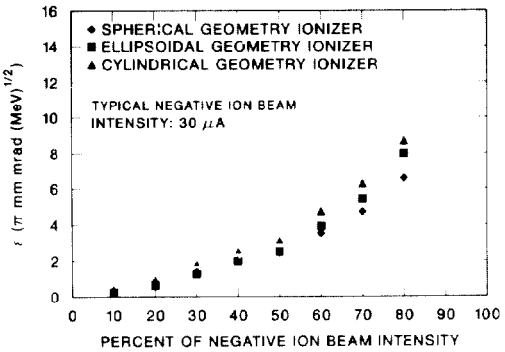

Fig. 5. Average normalized emittance ε versus percent total negative ion beam for the negative ion sources equipped with spherical (Ref. 3), ellipsoidal (Ref. 17), and cylindrical (Ref. 2) geometry cesium surface ionizers.

Plasma Sputter Negative Ion Sources

The advantage of the plasma-type source lies in the fact that, when operated in a high-density plasma mode, the negatively biased sputter probe containing the material of interest is uniformly sputtered. The plasma discharge in this type of source is usually formed from a heavy noble gas (Ar, Kr, or Xe) seeded with cesium vapor. This characteristic makes it possible to take advantage of the large area spherical geometry optics which occur between the spherical sector sputter probe and the plasma sheath surrounding the probe. Negative ions created in the process are accelerated and focused through the plasma to a common focal point which is usually chosen as the ion exit aperture. Thus, high beam intensities can often be realized while preserving a reasonable emittance value.

The radial geometry plasma sputter source

An example of a plasma-type source is that described in Ref. 4. In this source, which embodies some of the principles associated with the radial geometry source developed by Tykesson and Andersen[18], a weak magnetic field (~ 150 G) is used to collimate the primary electron beam which is thermonically emitted by a tantalum filament located at the end of the ionization chamber. The electron beam produces an approximately uniform plasma by collisional impact with neutral cesium vapor introduced into the chamber from the externally mounted oven. Auxiliary discharge support gas (usually Ar) is introduced into the chamber to supplement the cesium vapor; chemically active gases may also be introduced into the chamber for generation of atomic negative ions from the gas itself or for chemical combination with the sputter probe material in the formation of molecular negative ions. The sputter sample is

cylindrical (typically, 10 mm in diameter) with a concave spherical negative ion emission surface machined into the face of the material of radius ρ = 15 mm. The sputter probe is maintained at ~ −1000 V relative to the discharge chamber.

Examples of computational simulation of the negative ion optics as predicted by use of the code described in Ref. 16 are shown in Fig. 6.

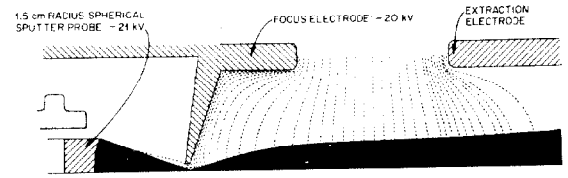

Fig. 6. Negative ion optics of the radial geometry cesium plasma source (Ref. 4).

Negative ion beam intensity data: Among the ions and intensities that have been reported are the following: 175 μA H^-, 0.4 μA Li^-, 4 μA BeH_3, 25 μA BeO^-, 0.6 μA B^-, 20 μA C^-, 20 μA C_2, 30 μA O^-, 20 μA F^-, 12 μA S^-, 12 μA MgH_3^-, 20 μA Si^-, 20 μA F^-, 2.5 μA Al^-, 9 μA Al_2^-, 2 μA CaH_3, 2.5 μA TiH_3, 55 μA Ni^-, 50 μA Cu^-, ~ 1 μA SrH_3, 35 μA Ag^-, 3.1 μA TaN^-, 1.4 μA W^-, 80 μA Au^-, and 7 μA PbN^-.

Emittance data: The normalized emittance (as defined by Eqs. 6) versus percent total negative ion beam current for a 48 μA $^{58}Ni^-$ ion beam is shown in Fig. 7. More detailed information concerning the emittance of this source is given in Ref. 18.

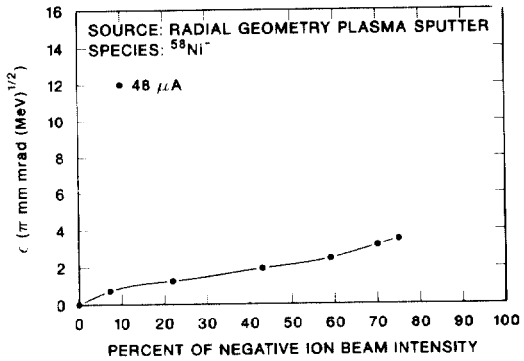

Fig. 7. Normalized emittance ε versus percent total negative ion beam for the radial geometry source described in Ref. 4. The total beam for this measurement was 48 μA ^{58}Ni.

The High-Intensity Plasma Sputter Negative Ion Source

The multi-cusp magnetic field plasma surface source, routinely employed for the production of high-intensity, pulsed H^- ion beams at LAMPF[19] and at the National Laboratory for High Energy Physics[20] has recently been modified for use as a high-intensity pulsed-mode heavy negative ion source.

For heavy negative ion generation, a high-density plasma discharge, seeded with cesium vapor, is produced by pulsing the discharge voltage of two series connected LaB_6 cathodes. In order to produce higher heavy negative ion beam intensities by sputter ejection at a given probe voltage, a chemically inert, heavy discharge support gas such as Ar, Kr, or Xe, is utilized. Cesium is introduced into the discharge from an external cesium oven. The sheath surrounding the negatively biased sputter probe (spherical radius, ρ = 140 mm and diameter, ϕ = 50 mm) which is made of the material of interest and is maintained at a negative voltage relative to housing, (typically, 500 to 2000 V) serves as the acceleration gap and lens for focusing the ion beam through the exit aperture (diameter, ϕ = 18 mm). When operated in the pulsed mode, the source holds considerable promise for use in conjunction with tandem electrostatic accelerator/synchrotron injection applications for heavy ion research. To date, the source has principally been tested in a low-duty-cycle (repetition rate: 1-50 Hz) macropulsed mode (pulse width: 50-300 μs). Computational simulation of the optics of this source for heavy negative ion generation using the code described in Ref. 16 is displayed in Fig. 8 for 3.5 mA O^- and 1 mA Au^- ion beams.

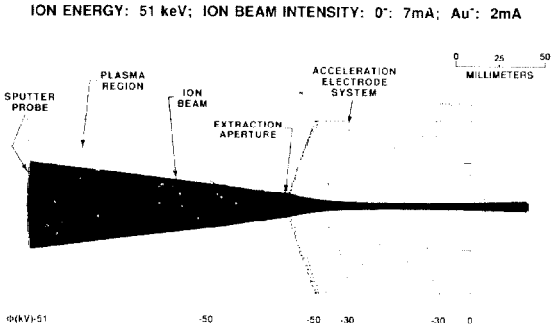

Fig. 8. Negative ion optics of the high-intensity plasma sputter heavy negative ion source described in Ref. 5.

Negative ion beam intensity data: Table 1 provides a partial list of total beam intensities, species, and probe materials utilized during operation of the source in pulsed mode. It should be noted that the peak negative ion beam intensities are frequently 100 times or more greater than the cesium surface ionization sources described previously.

Table 1. A partial list of total heavy negative ion beam intensities (peak) from the high-intensity plasma sputter heavy negative ion source.

Sputter Probe Material	Sputter Probe Voltage (V)	Geometry	Total Peak Beam Intensity (mA)	Species (%)
Ag	937	Spherical	6.2	Ag^- (91)
Au	437	Spherical	10.3	Au^- (73)
Bi	937	Spherical	2.7	Bi^- (6); O^- (42)
C	937	Spherical	6.0	C^- (36); C_2^- (58)
Co	937	Spherical	6.0	Co^- (85)
Cu	438	Spherical	8.2	Cu^- (77)
CuO	438	Flat	4.5	Cu^- (40); O^- (60)
GaAs	937	Flat	3.7	As^- (20); As_2 (52)
GaP	937	Flat	1.8	P^- (44)
Mo	438	Spherical	30.0	O^- (67)
Ni	438	Spherical	6.0	Ni^- (87)
Pd	937	Spherical	7.6	Pd^- (69)
Pt	937	Spherical	8.1	Pt^- (71)
Si	937	Spherical	6.0	Si^- (75)
Sn	937	Spherical	3.6	Sn^- (67)

Emittance data: Examples of beam emittances versus percent total negative ion beam are shown in Fig. 9 for Ni beams with peak pulse intensities of 2.5 and 6 mA. The emittances are seen to increase in proportion to the ion beam intensity as expected from space charge considerations. At the 80% contour level, the emittance values are comparable to those for the sources described previously when operated in the pulsed mode,[21] yet the beam intensities are often 100 times greater.

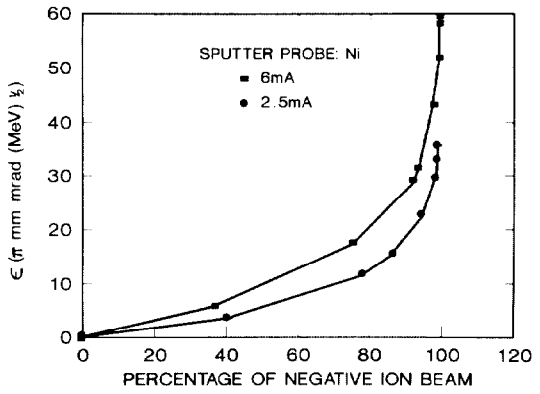

Fig. 9. Normalized emittance ε versus percent total negative ion beam for the high-intensity, plasma-sputter, negative ion source described in Ref. 5.

Conclusion

In recent years, considerable progress has been made toward a quantitative understanding of the mechanisms underlying negative ion formation during sputtering of a surface covered with small amounts ($\leq$ 1 monolayer) of a highly electropositive adsorbate material such as cesium. The development of models such as described in this paper have moved experiment and theory to closer agreement. There is, however, a need for additional experimental data before a proper assessment of the validity of models such as the one proposed by Nørskov and Lundqvist[10] can be made.

The sputter principle has proved to be a simple and almost universal method for efficient formation of negative ion beams from chemically active elements. Heavy negative ion sources predicated on this principle, such as described in this report, continue to be improved in terms of intensity and beam quality. Recent advancements in sputter ion source technology are exemplified by the high intensity pulsed mode plasma sputter source[5] which can produce intensity levels of several mA from a wide spectrum of negative ion species.

Acknowledgements

The author is especially indebted to Dr. Yoshiharu Mori, Mr. Akira Takagi, Dr. Akira Ueno, and Professor Sadayoshi Fukumoto of the proton/synchrotron group, National Laboratory for High Energy Physics, Tsukuba, Japan, for their cooperation and assistance in evaluating the multi-cusp magnetic-field H^- source as a source of heavy negative ions. The author also extends his appreciation to Ms. Jeanette McBride for typing and to Dr. C. M. Jones for editing the manuscript.

References

[1] R. Middleton, Nucl. Instrum. and Meth. **214** (1983) 139.
[2] G. D. Alton, Nucl. Instrum. and Meth. **A244** (1986) 133.
[3] G. D. Alton and G. D. Mills, IEEE Trans. Nucl. Sci. **NS-32** (5) (1985) 1822.
[4] G. D. Alton, R. M. Beckers, and J. W. Johnson, Nucl. Instrum. and Meth. **A244** (1986) 148.
[5] G. D. Alton, Y. Mori, A. Takagi, A. Ueno, and S. Fukumoto, Nucl. Instrum. and Meth. **A270** (1988) 194. Y. Mori, G. D. Alton, A. Takagi, A. Ueno, and S. Fukumoto, Nucl. Instrum.and Meth. **A273** (1989) 5.
[6] D. K. Olsen, G. D. Alton, S. Datz, P. F. Dittner, D. T. Dowling, D. L. Haynes, E. D. Hudson, J. W. Johnson, I. Y. Lee, R. S. Lord, C. A. Ludemann, J. A. Martin, J. B. McGrory, F. W. Meyer, P. D. Miller, W. T. Milner, S. W. Mosko, P. L. Pepmiller, and G. R. Young, Nucl. Instrum. and Meth. **B24/B25** (1987) 26.
[7] V. E. Krohn, Jr., Appl. Phys. **38** (1962) 3523.
[8] M. L. Yu, Phys. Rev. Lett. **40** (1978) 574.
[9] P. Sigmund, Phys. Rev. **184** (1969) 383.
[10] J. K. Nørskov and B. I. Lundqvist, Phys. Rev. **B19** (1979) 5661.
[11] M. L. Yu, Phys. Rev. Lett. **47** (1981) 1325.
[12] M. W. Thompson, Philos. Mag. **18** (1968) 377.
[13] A. Becker, Phys. Rev. **28** (1926) 341.
[14] G. D. Alton, Surf. Sci. **175** (1986) 226.
[15] W. B. Herrmannsfeldt, SLAC Rep. No. 166 (1973).
[16] J. H. Whealton, Nucl. Instrum. and Meth. **189** (1981) 55.
[17] G. D. Alton, J. W. McConnell, S. Tajima, and G. J.Nelson,Nucl. Instrum. and Meth. **B24/25** (1987) 826. G. D. Alton, Proc. 11th Symp. on Ion Sources and Ion-Assisted Technology, Tokyo, Japan (1987) 157. G. D. Alton and J. W. McConnell, Nucl. Instrum. and Meth. **A268** (1988) 445.
[18] P. Tykesson, H. H. Andersen, and J. Heinemeier, IEEE Trans. Nucl. Sci. **NS-23** (2) (1976) 1104.
[19] R. L. York and R. R. Stevens, Proceedings of the Third International Conference on Production of Negative Ions and Beams, edited by Krysto Prelec. (American Institute of Physics Conference Proceedings No. 111, New York, 1984) p. 410.
[20] Y. Mori, A. Takagi, K. Ikegami, and S. Fukumoto, Proceedings of Fourth International Conference on Production and Neutralization of Negative Ions and Beams, edited by James G. Alessi. (American Institute of Physics Conference Proceedings No. 158, New York, 1987) p. 378.
[21] G. D. Alton, Phys. Div. Progress Report, ORNL-6420, September 30, 1987, p. 222.